Journal of Crystallization Process and Technology, **2012, 2, 16-20**
http://dx.doi.org/10.4236/jcpt.2012.21003 Published Online January 2012 (http://www.SciRP.org/journal/jcpt)

Synthesis and Characterization of $CaPd_3O_4$ Crystals

Hiroaki Samata[1*], Satoshi Tanaka[1], Soichiro Mizusaki[2], Yujiro Nagata[2], Tadashi C. Ozawa[3], Akira Sato[4], Kosuke Kosuda[4]

[1]Graduate School of Maritime Sciences, Kobe University, Kobe, Japan; [2]College of Science and Engineering, Aoyama Gakuin University, Sagamihara, Japan; [3]International Center for Materials Nanoarchitectonics, National Institute for Materials Science, Tsukuba, Japan; [4]Materials Analysis Station, National Institute for Materials Science, Tsukuba, Japan.
Email: [*]samata@maritime.kobe-u.ac.jp

Received November 15th, 2011; revised December 21st, 2011; accepted December 29th, 2011

ABSTRACT

A new method for the crystal growth of alkaline-earth palladate $CaPd_3O_4$ was developed. The crystals were synthesized on a voltage-applied electrode in a molten chloride solvent. The maximum length of the crystal was about 1.5 mm. The X-ray diffraction data were refined well by assuming a cubic structure of the space group $Pm\bar{3}n$, and the lattice constant a was 5.7471 (10) Å. The temperature dependence of the resistivity showed semiconductor-like characteristics with a very small activation energy E_a of 0.45 meV at low temperatures, and the resistivity at 300 K was 0.1 Ω·cm. The temperature dependence of the molar magnetic susceptibility showed the Curie-Weiss paramagnetic behavior with a small molar Curie constant C_{mol} of $5.0(1) \times 10^{-3}$ emu K/(mol·Oe), indicating the existence of localized spin moments.

Keywords: Single Crystal; Electrochemical Technique; $CaPd_3O_4$

1. Introduction

Alkaline-earth palladate $CaPd_3O_4$ has a cubic $NaPt_3O_4$-type structure and exhibits a semiconductor-like temperature-dependent resistivity [1,2]. Hase and Nishihara calculated the band structure of $CaPd_3O_4$ by the FLAPW method within LDA and suggested that $CaPd_3O_4$ is a potential excitonic insulator in which electrons and holes bind as excitons [3]. Ichikawa and Terasaki reported that $CaPd_3O_4$ was a degenerate semiconductor with a low carrier concentration [4]. Chemical substitution on insulating compounds occasionally produces interesting physical properties, and insulator-metal transitions have been observed in the $Ca_{1-x}Na_xPd_3O_4$ and $Ca_{1-x}Li_xPd_3O_4$ systems [2,4-6]. The aliovalent ion-substituted $CaPd_3O_4$ is considered to be a good representative of a thermoelectric material [4]. Thermoelectric energy conversion in solids has great potential as an energy-saving technology, but this type of conversion is not widely used due to the poor performance of the materials.

We have previously investigated the effects of aliovalent ion substitution on the properties of $SrPd_3O_4$, which is isostructural with $CaPd_3O_4$, and we observed the existence of insulator-metal transitions and bipolar conductivity [7,8]. In this system, the substitutions of Na^+ and Bi^{3+} for Sr^{2+} introduced hole and electron carriers, respectively. The power factor of $Sr_{1-x}Na_xPd_3O_4$ ($x \leq 0.2$) was not sufficient for practical use as a thermoelectric material, but increasing the amount of substitution and devising an appropriate synthesis method may enhance its thermoelectric performance [8].

A strategy for searching for novel thermoelectric materials was suggested by the analysis of single-crystal data for Ce-based compounds [9]. Moreover, the use of a high-quality single crystal was effective for practical applications of thermoelectric materials [10]; therefore, the development of new crystal growth techniques is important for practical use as well as for the theoretical analysis of thermoelectric materials.

The growth of $CaPd_3O_4$ crystals was previously attempted using the conventional flux method; potassium hydroxide was used as the flux, and the crystallographic properties were characterized [11]. However, no other study has investigated the crystal growth, and the intrinsic properties of this material have not been elucidated in detail. Electrosynthesis in a molten flux effectively prepares single crystals of transition metal oxides [12], and we recently reported the crystal growth of certain oxides on electrodes in molten chloride solvents [13]. In the current study, we describe the results of the synthesis and the characterization of $CaPd_3O_4$ crystals.

2. Experimental

Single crystals of $CaPd_3O_4$ were synthesized on the surface of voltage-applied platinum rods submerged in mol-

[*]Corresponding author.

ten chloride solvent. A schematic of the apparatus used for the crystal growth is shown in **Figure 1** of [13]. An alumina crucible with a capacity of 20 or 30 cc was used to hold the solvent, which was a mixture of $CaCl_2$ and NaCl. An appropriate amount of PdO powder (99.9%) was placed in the crucible, and the chloride mixture was layered over the PdO powder. The total amount of chlorides was 20 or 30 g, and the molar ratio of NaCl/$CaCl_2$ varied in the range of 0 to 5.3; a PdO to $CaCl_2$ molar ratio of 0.04 to 0.12 was used. The crucible was placed in an alumina container, and two parallel platinum rods (0.5 mm in diameter) were inserted into the solvent at a distance of 7 mm from each other. The container was covered by an alumina plate and placed in an electric furnace with an ambient atmosphere. The depositions were performed at a constant temperature in the range of 780˚C to 1050˚C, which accounted for the melting points of $CaCl_2$ (772˚C) and NaCl (801˚C). After the solvent was melted at each synthesis temperature, an electrical voltage in the range of 0.2 to 0.4 V was applied to the electrodes using a DC power supply. The synthesis was carried out over 48 to 96 hours; the applied voltage was then turned off, and the electrodes were quickly extracted from the molten solvent. The crystals were washed thoroughly in distilled water to remove the solvent from the surface of the crystals, which were then dried on a hot plate. Selected crystals were annealed at 500˚C for 7 days under flowing oxygen gas at 1 atm.

The chemical composition of the crystals was characterized by electron-probe microanalysis (EPMA; JEOL, JXA-8500F). The crystal structure was identified by single-crystal X-ray diffraction and powder X-ray diffraction. Single-crystal X-ray diffraction data were acquired on a Bruker SMART APEX S diffractometer equipped with a pyrolytic graphite incident monochromator and a CCD camera at room temperature. The crystal was mounted on a glass fiber, and X-rays were generated using a Mo target at 50 kV and 30 mA. A total of 3597 reflections were collected for the full sphere using a 0.3˚ ω-scan with a 40 s exposure. The crystal structure was solved by direct methods using SHELXS-97, and the structure was refined utilizing the SHELXL-97 software package, which used 130 unique reflections and 7 parameters [14]. Powder X-ray diffraction data were acquired using Cu Kα generated at 40 kV and 20 mA in a 2θ range of 20˚ - 80˚ at room temperature (Rigaku, RINT2000). The data were refined by the Rietveld method using the values obtained from the refinement of single-crystal X-ray diffraction data [15].

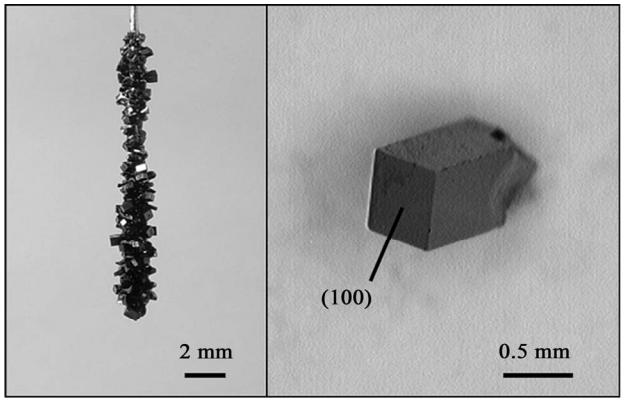

Figure 1. Photographs of as-grown $CaPd_3O_4$ crystals synthesized by applying a voltage of 0.2 V at 950˚C for 48 h: (a) crystals on the platinum anode rod and (b) a crystal removed from the electrode.

The electrical resistivity of the crystals was measured using a conventional DC two-probe method in the temperature range of 10 to 300 K; a refrigerator was used to maintain temperatures lower than room temperature. The electrical contacts were established by attaching gold leads onto the surface of the crystal using silver paste to form an ohmic contact. Magnetic measurements were carried out using a superconducting quantum interference device magnetometer (Quantum Design, MPMS2) in the temperature range of 5 to 300 K in an applied magnetic field of 10 kOe.

3. Results and Discussion

Figure 1(a) shows a photograph of the $CaPd_3O_4$ crystals grown by applying a voltage of 0.2 V at 950˚C for 48 hours; a molar ratio of PdO:$CaCl_2$:NaCl of 0.06:1:2 was used. The electrical current was approximately 1 mA at the end of crystal growth. These conditions were the most suitable for the growth of large crystals within the range of the present experimental conditions. Green-tinted black crystals grew on the surface of the anode. Because the crystals were grown in a molten flux, the natural surface of the crystal was observed, as shown in the photograph. **Figure 1(b)** shows a photograph of a crystal removed from the electrode. The maximum length of the crystal was about 1.5 mm. The EPMA measurements indicated that the Ca/Pd molar ratio of the as-grown crystal was 0.35. This value agrees with the calculated value of 0.33 that was assumed based on the chemical formula of $CaPd_3O_4$. The measured value of 0.35 did not vary in the direction of crystal growth. Because an alumina crucible, platinum electrodes, and chloride solvents were used in the synthesis, Al, Pt, Na, and Cl could have potentially been incorporated into the crystal; however, the EPMA measurements showed no inclusion of these elements. Tiny $CaPd_3O_4$ crystals also grew on the bottom of the crucible, but the size of each crystal was 0.01 mm or less, which is significantly smaller than the crystals grown on the anode. Based on this difference in size, we conclude that the application of the electrical voltage to the electrodes had a significant effect on the growth of large crystals. Because positive Pd ions

in the solvent were attracted by the cathode during the synthesis, the cathode was covered with metallic palladium. An increase in the amount of NaCl used in the synthesis resulted in a decrease in the amount of metallic palladium on the cathode; thus, NaCl seemed to inhibit the reduction of PdO.

The crystal structure of the $CaPd_3O_4$ crystal was characterized by the refinement of single-crystal XRD data, and the results are summarized in **Tables 1** and **2**. The data were refined well by assuming a cubic structure of the space group $Pm\bar{3}n$. The refined lattice constant a was 5.7471(10) Å, and this value agrees well with those reported in previous studies [1-2,4-6]. The crystal structure was also characterized by powder XRD. **Figure 2** contains the powder XRD profiles and the results of the refinement of the data. The data were refined well with reliability factors R_{wp} = 8.10, R_e = 8.07, and S = 1.004, and all peaks were indexed as a $NaPt_3O_4$-type structure. The refined a of 5.7471 Å is in fair agreement with that obtained by the refinement of the single-crystal XRD data. This result demonstrates that all crystals have the same structure. **Figure 3** shows the crystal structure of $CaPd_3O_4$. In this figure, palladium atoms are bonded with neighboring oxygen atoms; the distance between palladium and oxygen atoms is 2.0319(2) Å, and each palladium atom is surrounded by four coplanar oxygen atoms that form a PdO_4 square planar unit. These units are perpendicularly connected to each other via shared corner oxygen and form a three-dimensional framework. The large natural surface shown in **Figure 1(b)** was confirmed as the (100) plane of the cubic crystal.

Figure 4 shows the temperature dependence of electrical resistivity, which was measured for an as-grown crystal with a size of 0.103 × 0.130 × 0.647 mm^3. The current was flowed parallel to the [100] direction of a rectangular parallelepiped crystal. The resistivity showed semiconductor-like characteristics; the resistivity decreased as the temperature increased. The resistivity at 300 K was 0.10 Ω·cm. Because this measurement was performed with a single crystal, the result was free from the effects of the

Table 1. Crystallographic data and structure refinement data for $CaPd_3O_4$.

Formula weight	423.28 g/mol
Space group	$Pm\bar{3}n$ (No. 223)
a	5.7471(10) Å
V	189.822(6) Å^3
Z	2
Abs. coeff.	15.277 mm^{-1}
$F(000)$	380
Crystal size	80 μm × 80 μm × 40 μm
Final R indices $[I > 2\sigma(I)]$ [a]	$R1$ = 0.0199, $wR2$ = 0.0439
R indices (all data)	$R1$ = 0.0203, $wR2$ = 0.0445

[a] $R1 = \sum\left\|F_o\right| - \left|F_c\right\| / \sum\left|F_o\right|$; $wR2 = \left\{\sum\left[w\left(F_o^2 - F_c^2\right)^2\right] / \sum\left[w\left(F_o^2\right)^2\right]\right\}^{1/2}$, $w^{-1} = \left[\sigma^2\left(F_o^2\right) + \left(0.0077P\right)^2 + 1.34P\right]$, where $P = \left[\max\left(F_o^2, 0\right) + 2F_c^2\right]/3$.

Table 2. Atomic coordinates and isotropic displacement parameters (Å^2) for $CaPd_3O_4$.

	x	y	z	U_{iso}
Ca	0	0	0	0.0078(3)
Pd	1/4	0	1/2	0.0053(2)
O	1/4	1/4	1/4	0.0075(6)

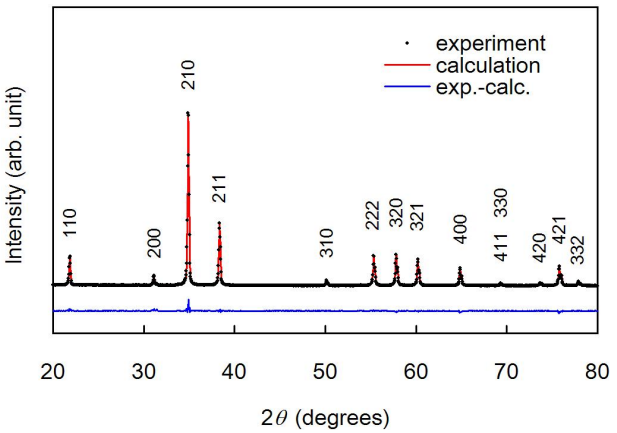

Figure 2. Powder X-ray diffraction profile of $CaPd_3O_4$ crystals and the results of refinement of the diffraction data by the Rietveld method.

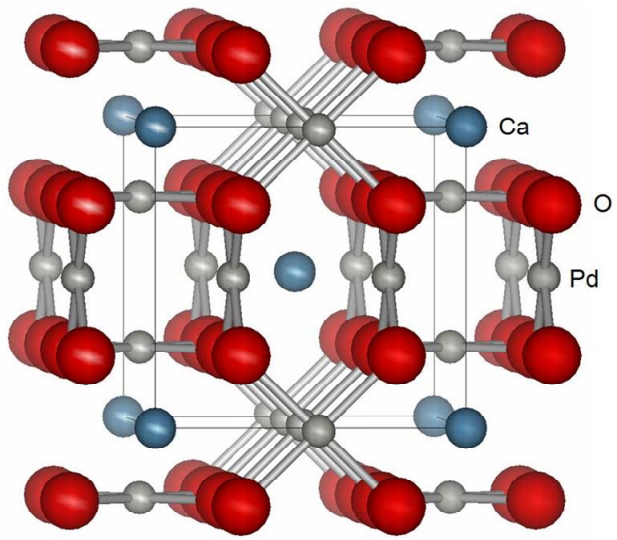

Figure 3. Crystal structure of $CaPd_3O_4$. Palladium atoms are bonded with four neighboring oxygen atoms, which are represented by gray bars. The solid line shows the unit cell.

grain boundary scattering. The inset of **Figure 4** shows an Arrhenius plot. The data at lower temperatures can be fitted by the thermal-activation process expressed by

$$\rho = \rho_0 \exp\left(\frac{E_a}{k_B T}\right), \quad (1)$$

where ρ_0, E_a, and k_B are the pre-exponential factor, the activation energy, and the Boltzmann constant, respectively. An E_a of 0.45 meV was obtained; this value is lower than that obtained for sintered material (1.1 meV) [2] and is inconsistent with the result of the band calculation, which predicted a semimetallic band structure with a zero band gap [3].

Figure 5 shows the temperature dependence of the molar magnetic susceptibility χ for as-grown crystals and the crystals annealed at 500˚C for 7 days under an oxygen atmosphere of 1 atm. The measurements were conducted in an applied magnetic field of 10 kOe during the heating process after zero-field-cooling (ZFC) and field-cooling (FC) process. The FC data were nearly identical to the ZFC data and are not shown. Both plots illustrate paramagnetic behavior with an increase of the susceptibility at low temperatures; χ can be fitted by the modified Curie-Weiss law expressed by

$$\chi = \chi_0 + \frac{C_{mol}}{T - \Theta}, \quad (2)$$

where χ_0, C_{mol}, and Θ are the temperature-independent magnetic susceptibility, the molar Curie constant, and the asymptotic Curie temperature, respectively. The solid line shows the results which were obtained by fitting the modified Curie-Weiss formula to the data, using the Marquardt-Levenberg algorithm [16]. The values $\chi_0 = -4.1(2)\times10^{-5}$ emu/(mol·Oe), C_{mol} = 5.0(1) × 10^{-3} emu K/(mol·Oe), and Θ = –1.4(2) K were obtained for the as-grown crystals. The effective number of the Bohr magneton per chemical formula unit p was calculated using the formula

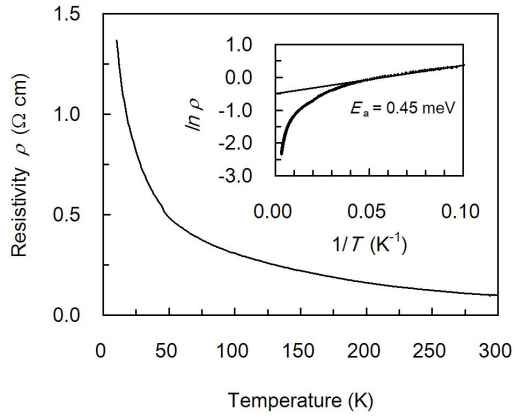

Figure 4. Temperature dependence of the electrical resistivity of an as-grown crystal. The inset of the figure shows the Arrhenius plot.

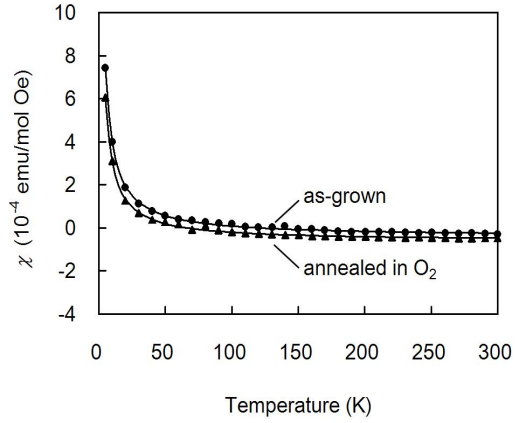

Figure 5. Temperature dependence of the molar magnetic susceptibility χ measured for as-grown crystals and oxygen-annealed crystals (10 kOe, ZFC).

$$C_{mol} = \frac{Np^2\mu_B^2}{3k_B}, \quad (3)$$

where N, μ_B, and k_B are the Avogadro constant, the Bohr magneton, and the Boltzmann constant, respectively. The value of p was determined to be 0.20/f.u. In $CaPd_3O_4$, Pd is the only magnetic ion. Based on the stoichiometry of the crystal, the valence of the Pd ion is 2+, and the electron configuration is $4d^8$. In this structure with PdO_4 tetragons, the $d_{x^2-y^2}$ energy level is the highest, and the d_{z^2}, d_{xy}, d_{yz}, and d_{zx} levels are filled by electrons in a low-spin configuration [8]. The band calculation also suggests that the empty $d_{x^2-y^2}$ forms the highest band [3]. Based on this configuration, diamagnetism was expected for $CaPd_3O_4$, and negative magnetic susceptibility was actually observed at a high temperature range; however, the Curie-Weiss paramagnetic contribution was observed, suggesting the existence of localized spin moments. Because the measurements were performed for single crystals, the Curie-Weiss paramagnetic behavior was not the effect of impurity magnetic phases. Because the paramagnetic contribution didn't decrease after the oxygen annealing of the crystals, the Curie-Weiss paramagnetic behavior was not the effect of the oxygen vacancies. The Curie-Weiss paramagnetic behavior is attributable to the existence of Pd^{3+}, which was induced by the existence of cation vacancies. As previously reported, the molar ratio of Ca/Pd was determined to be 0.35 by EPMA; this value is slightly larger than the value of 0.33 that is based on the stoichiometric composition. This disparity suggests that Pd vacancies are present, which would introduce Pd^{3+} in order to maintain the charge neutrality of the system [4,6,17]. In this case, the Curie-Weiss paramagnetic behavior would be induced by the unpaired spin at the d_{xy} level of Pd^{3+}; however, the exact cause of the Curie-Weiss paramagnetic behavior remains unclear at present.

4. Conclusion

Single crystals of alkaline-earth palladate $CaPd_3O_4$ were grown by an electrochemical technique that used voltage-applied platinum electrodes inserted into a molten chloride solvent. Crystals with natural surfaces were obtained on the anode, reflecting that the growth proceeded in a liquid phase. The maximum length of the crystal was about 1.5 mm. The crystal structure parameters were refined well by assuming a cubic structure of the space group $Pm\bar{3}n$, and the lattice constant a was 5.7471(10) Å. The resistivity showed semiconductor-like characteristics with a very small activation energy E_a of 0.45 meV at lower temperatures. The temperature dependence of the molar magnetic susceptibility showed the Curie-Weiss paramagnetic behavior, indicating the existence of localized spin moments.

5. Acknowledgements

The work performed at Kobe University and Aoyama Gakuin University was supported by Grants-in-Aid for Scientific Research from the Ministry of Education, Culture, Sports, Science and Technology of Japan.

REFERENCES

[1] R. C. Wnuk, T. R. Touw and B. Post, "The Crystal Structure of $CaPd_3O_4$," *IBM Journal of Research and Development*, Vol. 8, No. 2, 1964, pp. 185-186. doi:10.1147/rd.82.0185

[2] K. Itoh and N. Tsuda, "Metal to Semiconductor Like Transition for Sintered $Ca_{1-x}Na_xPd_3O_4$," *Solid State Com- munications*, Vol. 109, No. 11, 1999, pp. 715-719. doi:10.1016/S0038-1098(98)00549-3

[3] I. Hase and Y. Nishihara, "$CaPd_3O_4$, as an Excitonic Insulator," *Physical Review B*, Vol. 62, No. 20, 2000, pp. 13426-13429. doi:10.1103/PhysRevB.62.13426

[4] S. Ichikawa and I. Terasaki, "Metal-Insulator Transition in $Ca_{1-x}Li_xPd_3O_4$," *Physical Review B*, Vol. 68, 2003, p. 233101. doi:10.1103/PhysRevB.68.233101

[5] K. Itoh, Y. Yano and N. Tsuda, "Metal to Insulator Transition for $Ca_{1-x}Na_xPd_3O_4$," *Journal of the Physical Society of Japan*, Vol. 68, No. 9, 1999, pp. 3022-3026. doi:10.1143/JPSJ.68.3022

[6] Y. Yano, M. Kanazawa, T. Fujii and N. Tsuda, "Magnetic Susceptibility of $Ca_{1-x}Na_xPd_3O_4$," *Journal of the Physical Society of Japan*, Vol. 70, No. 6, 2001, pp. 1772-1176. doi:10.1143/JPSJ.70.1772

[7] T. Taniguchi, Y. Nagata, T. C. Ozawa, M. Sato, Y. Noro, T. Uchida and H. Samata, "Insulator-Metal Transition Induced in $Sr_{1-x}Na_xPd_3O_4$ for Small Na-Substitutions," *Jour- nal of Alloys and Compounds*, Vol. 373, No. 1-2, 2004, pp. 67-72. doi:10.1016/j.jallcom.2003.11.004

[8] T. C. Ozawa, A. Matsushita, Y. Hidaka, T. Taniguchi, S. Mizusaki, Y. Nagata, Y. Noro and H. Samata, "Synthesis and Characterization of Electron and Hole Doped Ternary Palladium Oxide: $Sr_{1-x}A_xPd_3O_4$ (A = Na, Bi)," *Journal of Alloys and Compounds*, Vol. 448, No. 1-2, 2008, pp. 77-83. doi:10.1016/j.jallcom.2007.03.137

[9] J. Kitagawa, T. Sasakawa, T. Suemitsu, Y. Echizen and T. Takabatake, "Effects of Valence Fluctuation and Pseudogap Formation on Phonon Thermal Conductivity of Ce-Based Compounds with ε-TiNiSi-Type Structure," *Physical Review B*, Vol. 66, No. 22, 2002, p. 224304. doi:10.1103/PhysRevB.66.224304

[10] A. Saramat, G. Svensson, A. E. C. Palmqvist, C. Stiewe, E. Mueller, D. Platzek, S. G. K. Williams and D. M. Rowe, "Large Thermoelectric Figure of Merit at High Temperature in Czochralski-Grown Clathrate $Ba_8Ga_{16}Ge_{30}$," *Journal of Applied Physics*, Vol. 99, No. 2, 2006, p. 023708. doi:10.1063/1.2163979

[11] P. L. Smallwood, M. D. Smith and H.-C. zur Loye, "Flux Synthesis of Alkaline Earth Palladates," *Journal of Crystal Growth*, Vol. 216, No. 1-4, 2000, pp. 299-303. doi:10.1016/S0022-0248(00)00432-2

[12] T. N. Nguyen and Hans-Conrad zur Loye, "Electrosynthesis in Hydroxide Melts," *Journal of Crystal Growth*, Vo. 172, No. 1-2, 1997, pp. 183-189. doi:10.1016/S0022-0248(96)00726-9

[13] H. Samata, Y. Saeki, S. Mizusaki, Y. Nagata, T. C. Ozawa and A. Sato, "Electrochemical Crystal Growth of Perovskite Ruthenates," *Journal of Crystal Growth*, Vol. 311, No. 3, 2009, pp. 623-626. doi:10.1016/j.jcrysgro.2008.09.042

[14] G. M. Sheldrick, SHELXTL, Version 6.10, Bruker AXS Inc., Madison, 1997.

[15] F. Izumi and T. Ikeda, "A Rietveld-Analysis Programm RIETAN-98 and Its Applications to Zeolites," *Materials Science Forum*, Vol. 321-324, 2000, pp. 198-205. doi:10.4028/www.scientific.net/MSF.321-324.198

[16] W. H. Press, B. P. Flannery, S. A. Teukolsky and W. T. Vetterling, "Numerical Recipes," Cambridge University Press, Cambridge, 1986.

[17] S. J. Kim, S. Lemaux, G. Demazeau, J. Y. Kim and J. H. Choy, "$LaPdO_3$: The First Pd^{III} Oxide with the Perovskite Structure," *Journal of the American Chemical Society*, Vol. 123, No. 42, 2001, pp. 10413-10414. doi:10.1021/ja016522b

